ELSEVIER

International Journal of Industrial Ergonomics 24 (1999) 141–155

International Journal of
Industrial
Ergonomics

Computer motion simulation for sagittal plane lifting activities

C.J. Lin[a], M.M. Ayoub[b,*], T.M. Bernard[c]

[a] *Department of Industrial Engineering, Chung Yuan Christian University, Chung Li, Taiwan, ROC 32023*
[b] *Department of Industrial Engineering, Texas Tech University, Lubbock, TX 79409-3061, USA*
[c] *Department of Occupational Safety and Health, Murray State University, Murray, KY42071-0009, USA*

Received 26 September 1997; received in revised form 15 December 1997; accpeted 16 December 1997

Abstract

In ergonomics, the biomechanical approach provides estimation of various mechanical stresses acting on the body while a person manually handles an object. Although motion analysis systems are available for dynamic biomechanical analyses, the use of such systems are mostly performed in laboratory due to high cost of the equipment and the expertise required in using them. Industrial ergonomists have limited access to dynamic biomechanical analyses. This paper reports a dynamic simulation model developed for biomechanical analyses of lifting activities performed in the sagittal plane. The model simulates the dynamic motion of lifting tasks for five body joints: the elbow, shoulder, hip, knee, and ankle. The inputs of the model include initial and final joint postures; gender, weight, and height; weight of load; lifting height; and container dimensions. In the output, the angular trajectories of the five joints are predicted. The model without any video inputs predicts the motion patterns of the lift. Actual motion data were collected using 10 subjects in the laboratory for 360 lifts which included 12 lifting tasks in combination of two lifting heights, two container sizes, and three weights of load. Good results were found for the dynamic planar motion simulation model. The predicted motion pattern from the simulation closely resembles the observed motion pattern.

Relevance to industry

The lifting motion simulation model reported in this paper can be used to predict motions for various sagittal plane lifting tasks. The motion profiles can then be used in the dynamic biomechanical analysis without having to obtain the filmed motion. This allows field industrial ergonomists to perform better job analysis involving dynamic models.

Keywords: Dynamic biomechanical models; Motion simulation; Sagittal plane lifting activities; Kinematics; Kinetics; Optimization; Trajectory

* Corresponding author.

0169-8141/98/$ - see front matter
PII: S0169-8141(98)00010-9

1. Introduction

In ergonomics, biomechanical studies of manual lifting represent a major area of interest. To estimate stresses imposed on the body's musculoskeletal system while lifting, especially forces at major joints and the lumbar spine, two or three-dimensional whole-body biomechanical models are usually used. Since Chaffin (1969) published the use of the "static sagittal plane" model for studying whole-body load lifting, and later popularized it with the Static Strength Prediction Program (The University of Michigan), the software has become a useful tool for industrial ergonomists to analyze, design, and modify jobs. One of the concerns in using the results predicted from static biomechanical models is that the imposed body stresses from performing dynamic manual tasks tend to be underestimated and the strength capacities of the body overestimated due to the neglect of inertial forces. Studies have shown that in estimating stresses on the body, inertial forces can be substantial (Garg et al., 1982; Leskinen, 1985). To more accurately estimate body stresses during a lift, dynamic biomechanical analyses are usually recommended. The basic input for a dynamic lifting analysis is a complete time-history of the body's motion. To obtain motions of lifting, photographic or optical motion acquisition systems are usually used. Unfortunately, the cost of these systems are relatively high and the operation of the equipment requires certain expertise. Also, the data reduction procedure requires much time and can be very tedious. The major use of such method remains in the laboratory. Field industrial ergonomists who recognize the importance of the dynamics of MMH activities have limited access to dynamic analyses.

Techniques in human motion synthesis can be used to generate motions using a computer. These techniques thus provide the means for ergonomists to perform dynamic biomechanical analyses without actually collecting time–displacement data.

Early motion simulation efforts started with a single or a few segments, such as the upper or lower extremities with limited degrees of freedom in motion (Ayoub, 1971; Townsend and Seireg, 1972; Petruno, 1972). With the advanced power of computing, whole-body motion modeling with more degrees of freedom became available. Hatze (1981) used a 17-segment model with 46 major muscle groups to simulate the dynamics of the long jump. This model had 42 degrees of freedom. Yamaguchi (1990) used a three-dimensional stick man model to simulate human gait motion. The model consisted of a trunk and legs with 8 degrees of freedom and 10 muscles. Badler et al. (1993) developed a model capable of generating various human motions. As for the motions of lifting activities, the earliest motion prediction model can be traced back to Muth (1976) and Muth et al. (1978), in which a nonlinear optimization model was proposed to evaluate lifting tasks. Lee (1988) proposed a similar optimization model to determine lifting motion. The position trajectories of the body joints were considered to be discrete points in time and dynamic programming was used to find the optimal motion. Based on similar models, Hsiang and Ayoub (1994) developed a model using a more efficient solution method based on eighth-order polynomials and nonlinear optimization techniques. The simulation methodology proposed in Hsiang and Ayoub (1994) has been extensively expanded and further developed. This paper presents the development of the dynamic planar motion simulation (DPMS) model and the results of the simulation performed on various lifting tasks.

2. Model description

The DPMS model has the capability to predict the joint motion trajectories for lifting activities in the sagittal plane, provided that the starting and ending postures and the total duration of the lift are given. The model assumes that the human body performs a lifting task according to some criterion such as the minimization of the total muscular effort. While the body is trying to minimize the effort to complete the task, it is subject to various constraints such as the strength capability of the joints and the geometrical layout of the work place. The model takes as inputs the starting and ending postural configurations, weight of the load being lifted, subject anthropometric and body segment parameters, and time to complete the lift. In the output, a complete angular motion history of the

body joints is produced. Kinematic and kinetic analyses of the lift can be performed based on the predicted motion. The simulation model is composed of three sub-models. The following describes the sub-models used for the simulation.

2.1. The biomechanical model

The biomechanical model used in the simulation is a five-segment whole-body symmetrical lifting model. Fig. 1 shows the link-segment diagram of the model and the coordinate convention. The human body consists of the lower leg, upper leg, trunk, upper arm, and lower arm. The five joints under consideration are the elbow, shoulder, hip, knee, and ankle. The body's configuration at any moment in time can be completely specified by the angles of each segment with respect to the horizontal, $\theta_j, j = 1, \ldots, 5$. Fig. 2 shows the free-body diagram of a link-segment model. Given the weight of the load, inertial property of the segments, and length of the segments, joint forces and moments can be calculated by the following equations of motion:

$$\boldsymbol{R}_j - \boldsymbol{R}_{j-1} + m_j\boldsymbol{g} = m_j\boldsymbol{a}_j,$$

$$\boldsymbol{M}_j - \boldsymbol{M}_{j-1} - \boldsymbol{r}_{j-1,cmj} \times \boldsymbol{R}_{j-1} + \boldsymbol{r}_{j,cmj} \times \boldsymbol{R}_j = I_j\ddot{\theta}_j, \quad (1)$$

where

$\boldsymbol{R}_j$ = force vector acting at joint j to link j,
$\boldsymbol{M}_j$ = moment vector acting to link j about joint j,
$\boldsymbol{r}_{j,cmj}$ = linear position vector pointing from the center of mass of link j to joint J,
$\boldsymbol{a}_j$ = linear acceleration vector of the center of mass of link j,
$\ddot{\theta}_j$ = angular acceleration vector of link j,
$\boldsymbol{g}$ = gravity vector,
m_j = mass of link j,
I_j = moment of inertia of link j about an axis passing through the center of mass normal to the sagittal plane of motion,
$\times$ = vector (cross) product operator.

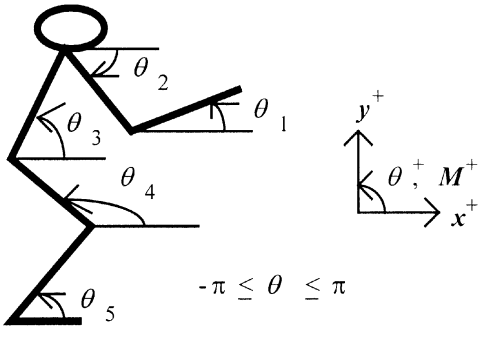

Fig. 1. The link-segment model of the lifting person.

2.2. The optimization model

In optimization theory, the objective function may be thought of as the cost function of the system and the constraints the available resources of the system. While the cost is being minimized, the

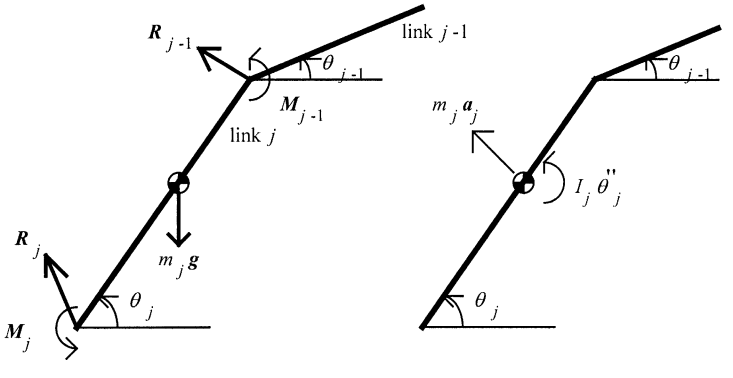

Fig. 2. The free-body diagram of a body link and its adjacent link.

resources are usually limited. The optimization lifting model assumes that the human body performs a lifting task according to some criterion such as the minimization of the total muscular effort. While the body is trying to minimize the effort to complete the task, it is subject to various constraints such as the strength capability of the joint and the geometrical layout of the work place. With the assumption, the lifting activity is formulated into a mathematical optimization problem with an objective function specifying the minimization of the effort, subject to various constraints.

The objective function is

$$\text{minimize} \int_{t=0}^{T} \sum_{j=1}^{5} \left(\frac{M_j(t)}{S_j(t)} \right)^2 \mathrm{d}t, \tag{2}$$

where

M_j = the magnitude of the moment about joint j,
S_j = the static moment strength of joint j,
T = total lifting time.

Since there is no population dynamic strength data available, static moment strength is used in the objective function. The static moment strength is predicted by equations from Stobbe (1982). The same objective function was used by Lee (1988) and Hsiang and Ayoub (1994) and was found to be robust in representing the total lifting effort in their simulation studies. Empirically, Fogleman and Smith (1995) found a decreasing trend in the value of the objective function when subjects performed extended periods of lifting tasks, indicating that the objective function is linked to the physical effort a person exerts during a lift.

In optimization problems, constraints are used to control the amount of resources available to the system. Numerically, constraints serve to reduce the feasible solution space while searching for the optimal answer. The earlier model as in Hsiang (1992) used a large number of constraints including kinematic and kinetic constraints. The use of a large number of constraints with more complex forms than simple bounds increases the complexity of the optimization problem dramatically. Furthermore, if many nonlinear constraints are present, the problem is generally intractable, as pointed out by Shanno (1990). To avoid such problems, a new formulation of the constraints for the lifting optimization model was considered as follows:

(1) Joint mobility constraints

$$\alpha_{j,\mathrm{L}} \leqslant \alpha_j(t) \leqslant \alpha_{j,\mathrm{U}}, \quad j = 1, \ldots, 5, \quad 0 \leqslant t \leqslant T \tag{3}$$

where

$\alpha_j(t)$ = included angle of joint j at time t,
α_j,L = minimum included angle of joint j,
α_j,U = maximum included angle of joint j.

The joint included angle, α, is defined as the relative angle between the two adjacent links connected by that joint. The included angle describes the joint rotational mobility in two directions. For example of the shoulder joint, in the standing posture, the entire arm can rotate 180° forward in the sagittal plane relative to the trunk; however, backward rotation can only reach about 60°. The maximum included angle is the maximum rotational angle in one rotational direction and the minimum included angle the maximum rotational angle in the other direction with a negative sign. The following equations describe the relationships between α and θ:

$$\begin{aligned} \alpha_1 &= \pi - \theta_1 + \theta_2, \\ \alpha_2 &= \pi - \theta_3 + \theta_2, \\ \alpha_3 &= \pi - \theta_4 + \theta_3, \\ \alpha_4 &= \pi - \theta_4 + \theta_5, \\ \alpha_5 &= \theta_5. \end{aligned} \tag{4}$$

Table 1 presents the joint included angle boundaries used in the DPMS model. These boundary values are converted from the joint mobility (flexion and extension) data provided in Chaffin and Andersson (1991). Note that the data represents the mean ranges for young healthy males. For the DPMS model, these ranges are assumed for both males and females. It is worth noting that

Table 1
Ranges of joint included angles, in degrees

Joint	Lower bound	Upper bound
Elbow	38	180
Shoulder	− 61	188
Hip	67	180
Knee	67	180
Ankle	55	90

both Lee (1988) and Hsiang (1992) used joint angular position constraints. The boundaries for the angular positions θ were derived from the actual kinematic data collected in their studies. Setting limits on θ of each joint independently does not restrict the relationship between the two links. It is possible for the elbow to over-extend while the joint angular positions are well within bounds.

(2) Joint moment strength constraints

$$M_j(t) \leqslant S_j(t), \quad j = 1, \ldots, 5 \tag{5}$$

where

S_j = the moment strength of joint j, as predicted by Stobbe's (1982) equations,

M_j = the magnitude of the moment vector M_j at joint j.

The constraints on joint moments describe the strength-limited behavior of human motion. In the previous model, Hsiang and Ayoub (1994) used velocity, acceleration, and jerk (rate of change of acceleration) constraints by specifying simple bounds for these parameters. The use of the kinematic constraints was not adopted in the present study for two reasons. First, using the higher-order kinematics constraints increases the number of constraints dramatically. As mentioned earlier, this tends to make the optimization problem much more complex. Second, it was felt that the joint moment strength should be the dominating limiting factor for the entire motion. In dynamics theory, if we are given the motions of a system, we can deduce the forces and moments acting. Conversely, given the forces and moments, we can solve for the motions (Greenwood, 1988). The kinematics and kinetics are tightly coupled by the equations of motion. For human motion, the kinematics can be viewed as a result of the kinetics, that is, the motion is driven by the forces and moments the body exerts. The constraints specified by the bounds of the kinematics parameters are in theory already governed by the kinetic constraints. Thus, the kinematics constraints are redundant when the kinetic constraints are present.

(3) Collision avoidance constraints

$$\text{if} \left\{ y_{\text{box}}(t) \in \left[y_{\text{shelf}} - \left(\frac{h}{2} + \delta \right), y_{\text{shelf}} + \left(\frac{h}{2} + \delta \right) \right] \right\}$$

$$\text{then} \left\{ \left[x_{\text{box}}(t) + \frac{l}{2} + \delta \right] - x_{\text{shelf}} < 0 \right\} \tag{6}$$

$$\text{if} \left\{ y_{\text{knee}}(t) \in \left[y_{\text{box}}(t) - \left(\frac{h}{2} + \delta \right), y_{\text{box}}(t) + \left(\frac{h}{2} + \delta \right) \right] \right\}$$

$$\text{then} \left\{ \left[x_{\text{box}}(t) - \frac{l}{2} \right] - [x_{\text{knee}}(t) + \delta] > 0 \right\}, \tag{7}$$

where

$(x_{\text{box}}(t), y_{\text{box}}(t))$ = position of the center of box at time t,

$(x_{\text{knee}}(t), y_{\text{knee}}(t))$ = position of the knee joint at time t,

$(x_{\text{shelf}}, y_{\text{shelf}})$ = position of the edge of shelf,

h = height of box in the sagittal plane,

l = length of box in the sagittal plane,

T = total lifting time,

δ = collision tolerance.

Fig. 3 shows the geometric relationships between the person, the box, and the shelf. The position of the edge of the shelf $(x_{\text{shelf}}, y_{\text{shelf}})$, is known and is a model input. Eq. (6) describes the avoidance of collision between the box and the shelf. When there is nothing under the shelf, the box may go under the shelf during the lift; however, when the box is near the shelf, the person will avoid hitting the shelf. The equation indicates that when the center of the box is at a certain height within the range of $[y_{\text{shelf}} - (h/2 + \delta), \ y_{\text{shelf}} + (h/2 + \delta)]$, the frontal edge of the box, $(x_{\text{box}}(t) + l/2)$, must not move beyond the edge of the shelf, x_{shelf}, in order to avoid collision. Note that the collision tolerance, δ, is used to describe the clearance between the box and the shelf that is needed for the person to freely move the box around the edge of the shelf. Similarly, Eq. (7) indicates that when the height of the knee joint is within the upper and lower edges of the box,

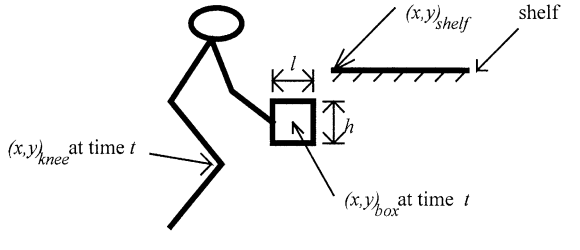

Fig. 3. Geometric relationships between the person, box, and shelf.

the horizontal position of the rear edge of the box should be greater than that of the knee plus a tolerance to avoid collision.

(4) Postural stability constraint

$$(X_{\text{heel}} + \delta) \leqslant x_{\text{cm}} \leqslant (x_{\text{toe}} + \delta), \tag{8}$$

where

x_{cm} = horizontal position of the system center of mass,
x_{heel} = horizontal position of the end of foot,
x_{toe} = horizontal position of the tip of foot,
δ = allowance for the thickness due to wearing shoes.

The postural stability constraint indicates that the horizontal position of the center of mass of the lifting system, including the person and the box, should not fall outside the foot support area. This constraint assumes a static situation for the lifting system, that is, it merely considers the balance as if the person is holding the box statically at each successive time frame. Furthermore, it assumes that the foot does not actively produce muscle moment to counterbalance the reactive moment acting about the ankle.

2.3. Trajectory models

Based on extensive studies on the trajectory patters of lifting motion from laboratory experiments, a curve-generating technique that employs polynomial functions of time has been found useful in approximating the actual trajectory. The following four assumptions were made for the trajectory model development:

1. All the joints are motionless when the lift begins and ends. In performing the lift, the subject starts with a static posture (initial posture) and ends at another static posture (final posture). When the lift starts, there might be subtle movements of each joint in different orders. It is difficult to define a common beginning and an end for all the joints; however, this assumption is in general true in terms of whole-body action.
2. The motion undergoes a constant number of acceleration peaks. For the same task condition, the number of peaks (or troughs) is constant in the acceleration trajectory; therefore, the number of peaks is also constant in the velocity and position trajectories. Here, the peaks are defined as the highest points in a curve where their derivatives are zero. For a natural lift, the motion is completed without stopping. The kinematic property of the motion can be characterized by these ups and downs in the motion trajectories.
3. The magnitudes of the acceleration (or velocity, position) peaks are bounded. The peaks in acceleration are bounded in part because of the limit in human strength. The peaks in position are bounded in part because of the geometrical layout of the task, such as the height of the shelf.
4. The times at which the acceleration (or velocity, position) peaks occurred are bounded. Lifting requires appropriate movement coordination between joints. To smoothly complete a lift, the timing of these peaks plays an important role. Inappropriate timing will result in an unnatural lift and sometimes a failure to complete the lift. The timing of these peaks is in part a result of the body configuration during the lift. For example, at the final stage of the lift, it is difficult to exert a large force to generate a high acceleration because the load is away from the body. A large moment arm is created for the load resulting in a mechanical disadvantage. Also, it is not necessary for a high acceleration to occur at this stage of the lift while one is trying to put the load down.

Based on the above four assumptions, a polynomial as a function of time t, $\theta(t)$, can be developed for each joint, that satisfies the following system of equations. The polynomial is then used to generate the angular trajectory.

$$\theta(0) + p_0, \tag{9}$$

$$\theta(T) = p_T, \tag{10}$$

$$\dot{\theta}(0) + \ddot{\theta}(0) + \dot{\theta}(T) = \ddot{\theta}(T) = 0, \tag{11}$$

$$\theta(t_i) = p_i,\ i = 1,2,\ldots,n, \tag{12}$$

$$\dot{\theta}(t_i) = 0,\ i = 1,2,\ldots,n. \tag{13}$$

In Eq. (9), p_0 is the initial angular position of the joint. In Eq. (10), p_T is the ending position of the joint and T is the total duration of the lift. The parameters p_0, p_T, and T are given inputs. In Eq. (11), the velocities and accelerations at times

zero and T are set to zero based on the assumption that the lift is performed with a motionless start and end. In Eqs. (12) and (13), p_i is the ith local peak or trough in the trajectory and t_i is the time when the ith peak or trough occurs. The parameter n is the total number of peaks or troughs in the trajectory for a joint and is determined from the actual trajectory. Eq. (13) holds because the velocity at the peak is zero. Fig. 4 shows a typical trajectory of the elbow joint with one peak point (p_1, t_1). Different joints have different number of peaks or troughs in their trajectories. The shape of the trajectory and therefore the kinematics properties of the joint described by that trajectory are controlled by the values of (p_i, t_i). For each joint, the polynomial trajectory models (9)–(13) that best fit the shapes and patterns of the actual trajectories have been developed. Given (p_i, t_i), the solution to the above system of equations is a Hermite polynomial of order $2n + 5$ (Atkinson, 1989). It can be shown that the solution exists and is unique. The values of (p_i, t_i) have been studied from the experimental data and were found to be located within a narrow region which made the patterns of the trajectory relatively similar across different lifts.

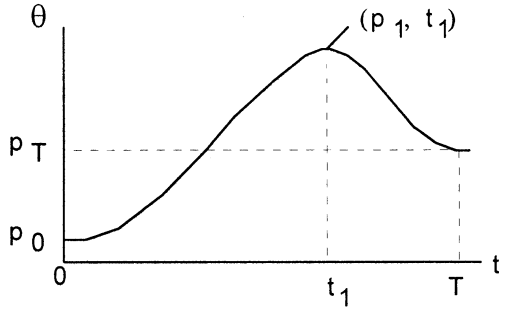

Fig. 4. A typical elbow trajectory with one peak point.

In the above derivation of a hypothetical trajectory, the initial and final positions, p_0 and p_T, are given as model inputs. They are subject to variation between lifts. The total lifting time, T, of each lift is a given input and subject to variation too. Two lifts may have a different T but their general pattern looks the same. Similarly, two lifts may have the same trajectory differed only by their initial and final positions. Fig. 5 shows that in one case two similar curves end at different times, and in another case the two are the same but merely separated by their initial and final positions. The following normalization scheme was therefore used in the development of the trajectory models for each joint:

$$\lambda = (\theta - p_0)/(p_T - p_0), \tag{14}$$

$$\tau = t/T, \tag{15}$$

where

λ = normalized angular position,
τ = normalized time, $0 \leqslant \tau \leqslant 1$,
θ = angular position,
t = time,
p_0 = initial position,
p_T = final position,
T = total lifting time.

The normalization is a rescaling of the coordinates in both the time and position scales. Using this normalization scheme, the peak position (p_1, t_1) in Fig. 4 will be transformed into normalized

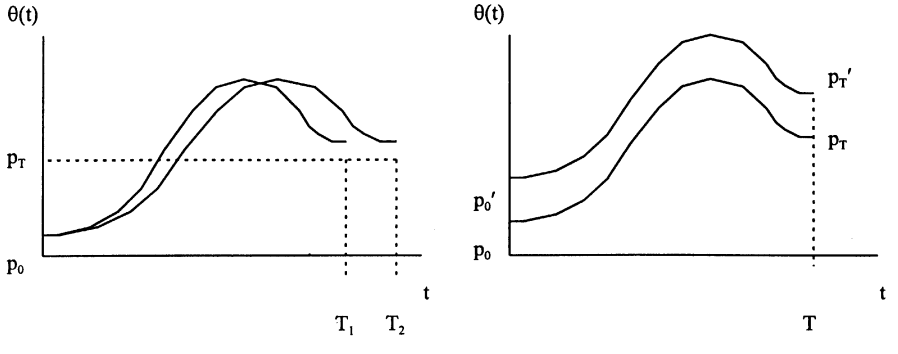

Fig. 5. Similar trajectories with different ending times (left) and different initial and final positions (right).

coordinates (λ_1, τ_1), bounced in normalized rectangle region. The use of normalized coordinates allows for a comparison between different lifts and possibly a generalization of motion patterns among different lifts.

3. Data collection

Lifting motion data were collected in the laboratory. The data provided inputs for the DPMS model such as the initial and final postural angles and total lifting time. The data were also used for the development of joint trajectory models for each joint. Five male and five female subjects were used in the data collection phase. Subject characteristics are presented in Table 2. The lifting conditions included two ranges of lift, floor-to-knuckle and floor-to-shoulder; three weights of lift, heavy, medium, and light; and two container sizes, large (45 cm × 30 cm × 30 cm) and small (30 cm × 30 cm × 30 cm). The large box had its length (45 cm) in the sagittal plane. The ranges of lift were adjusted to the subject's own knuckle and shoulder heights. For males, the three levels of weights were 11.4, 15.9, and 20.5 kg. For females, they were 4.5, 6.8, and 9.0 kg.

Prior to data collection, subjects practiced the lifting activities. Free-style lifts were performed. All twelve combinations of lifting conditions were practiced with one hour per condition. In the training session, two minutes were allowed for sufficient rest between lifts. The order of lifts was randomized. The initial location of the box on the floor was controlled. The box was placed on the floor at the same location for every lift, with the frontal edge of the box positioned directly beneath the edge of the shelf. A total of 360 lifts were performed by each subject in the training session.

During data collection, three replications were performed for each condition. The order of lifts was completely randomized within each subject. Reflective markers were attached to the body landmarks at the hand, elbow, shoulder, hip, knee, and ankle. The placement of the feet was controlled. Subjects selected their preferred locations of feet for the two box sizes and used them throughout the experiments. Prior to each lift, subjects stayed in a motionless static posture with their hands holding the handles of the box without applying any force. They were given an oral signal to start the lift and move the box from the floor to the shelf. Other conditions remained the same as in the training. The collection of data for the conditions for ten subjects with three replications resulted in a total of 360 lifts available for the simulation study.

The total duration of the filming time was sufficiently longer than the duration of the lift to cover the beginning and end of the lift. The beginning of the lift was defined as the time at which the box was completely lifted off the floor. The end of the lift was defined as the time at which the box was completely put down on the shelf. Electrical signals initiated instantaneously by the lift-off and landing

Table 2
Subject characteristics

Subject	1	2	3	4	5	6	7	8	9	10
Sex	f	f	f	m	f	m	m	f	m	m
Age	22	28	25	27	21	19	23	29	27	19
Height	1.71	1.7	1.62	1.75	1.73	1.83	1.68	1.57	1.76	1.93
Weight	59.5	69.1	50.9	69.5	70.4	80.9	79.1	80.9	65	90.9
Shoulder height	1.25	1.28	1.18	1.29	1.27	1.35	1.26	1.11	1.29	1.46
Knuckle height	0.62	0.63	0.53	0.63	0.61	0.64	0.63	0.51	0.62	0.69
Forearm	0.35	0.33	0.34	0.34	0.36	0.39	0.36	0.31	0.35	0.42
Upper arm	0.30	0.35	0.31	0.33	0.31	0.33	0.31	0.30	0.32	0.35
Trunk	0.51	0.56	0.45	0.52	0.55	0.56	0.51	0.48	0.47	0.56
Thigh	0.40	0.40	0.40	0.38	0.39	0.40	0.42	0.40	0.46	0.45
Lower leg	0.41	0.40	0.41	0.43	0.42	0.44	0.42	0.39	0.44	0.48

Note: The weight is in kilograms and length is in meters

of the box were sent to the Motion Analysis System and marked in the motion data record. The collected motion data were digitized and smoothed between the two time event marks. Analysis and modeling were based on the smoothed motion data.

4. Simulation method

The simulation method is characterized by the inverse dynamics approach where the angular trajectories of each joint are first generated and forces and moments calculated. Based on the kinematics and kinetics data calculated, the objective function and constraints can be calculated. The optimization is then implemented on a computer using an optimization software routine. Fig. 6 shows the structure of the simulation program consisting of three components: the trajectory formation, the biomechanics, and the optimization. The data flow between each component is depicted in the figure.

The angular joint trajectories are generated in the trajectory formation unit using the polynomial trajectory models described above. The trajectories are controlled by a set of control variables (p_i, t_i), that can be set at random initially, or set to average values obtained from the experimental data. The joint trajectories are then sent to the biomechanics unit where kinematics (velocity, acceleration) and kinetics (force, moment) of the joints and center of gravity are calculated based on the biomechanical model mentioned above. The Cartesian trajectories of the joints, container, and center of gravity are also calculated. These parameters are then sent to the optimization unit. The objective function and the constraints are functions of these parameters. The values of the objective function is then evaluated. Minimization of the objective function, subject to the constraints, is carried out with respect to the control variables of the joint trajectories. The optimization routine generates intermediate values of the control variables at each iteration. Using the intermediate values of the control variables, new joint trajectories are generated in the trajectory formation unit. New trajectories are sent to the biomechanics unit and the computation continues. The final solutions of the control variables given by

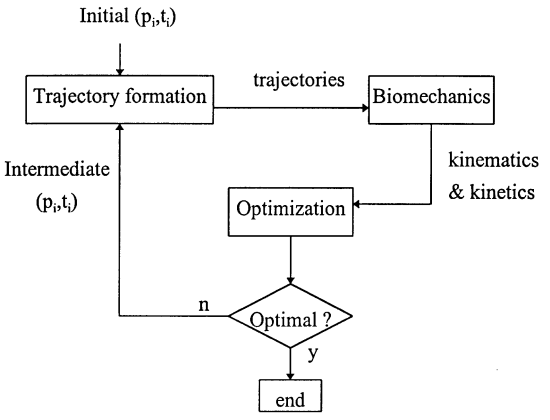

Fig. 6. The structure of the simulation program and data flow.

the optimization routine are used for the generation of optimal joint trajectories.

The GRG2 nonlinear optimization software (Lasdon and Waren, 1979, 1986), a general-purpose nonlinear optimization system, was used for the optimization. The GRG2 system is a widely distributed system and has been shown to be effective to deal with problems where the objective and constraint functions are both nonlinear (Subramanian and Hung, 1993).

5. Results and discussion

5.1. Trajectory characteristics and polynomial models

Initial and final velocities and accelerations of the joint angular trajectories were assumed as zero in the simulation model. To verify this assumption, initial and final joint velocities and accelerations were calculated for the 360 actual lifts. Table 3 shows the 95% confidence intervals from a student t-distribution for the means of the initial and final velocities and accelerations. Except the initial velocity at the shoulder, the 95% confidence intervals for the means of initial and final velocities and accelerations do not contain zero, indicating that for most joints, the initial and final velocities and accelerations were not zero. It must be noted that although the tests failed to show that the means of

Table 3
Confidence intervals for the means of initial and final velocities and accelerations ($N = 360$)

	Initial velocity (rad/s)			Final velocity (rad/s)		
Joint	mean	stdev	95% C.I.	mean	stdev	95%C.I.
Elbow	0.118	0.010	(0.099,0.137)	− 0.063	0.006	(− 0.075, − 0.51)
Shoulder	− 0.018	0.016	(− 0.045,0.014)	− 0.209	0.013	(− 0.234, − 0.184)
Hip	0.200	0.016	(0.169,0.232)	− 0.074	0.007	(− 0.087, − 0.061)
Knee	− 0.225	0.021	(− 0.266, − 0.183)	− 0.115	0.004	(− 0.124, − 0.107)
Ankle	0.261	0.009	(0.245,0.278)	− 0.114	0.005	(− 0.123, − 0.104)

	Initial acceleration (rad/s^2)			Final acceleration (rad/s^2)		
Joint	mean	stdev	95% C.I.	mean	stdev	95% C.I.
Elbow	0.566	0.061	(0.446,0.685)	0.860	0.059	(0.744,0.977)
Shoulder	− 2.160	0.092	(− 2.341, − 1.978)	− 0.735	0.103	(− 0.938, − 0.531)
Hip	1.545	0.090	(1.370,1.721)	1.415	0.044	(1.329,1.501)
Knee	− 2.894	0.103	(− 3.097, − 2.692)	− 0.171	0.018	(− 0.206, − 0.136)
Ankle	1.447	0.047	(1.355,1.539)	− 0.502	0.027	(− 0.555, − 0.448)

the initial velocities and accelerations were zero, their values were relatively close to zero when compared to the maximum velocities and accelerations in each lift. In general, the forms of a polynomial will not be completely altered by the use of some small initial or final velocities and accelerations. In the simulation model, zero initial and final velocities and accelerations were used, assuming that the actual initial and final velocities and accelerations were not available.

The normalization scheme in Eqs. (14) and (15) was applied to the actual joint trajectories to study the patterns of the trajectories across different lifts. A typical trajectory pattern was found for each joint across all lifting conditions and subjects. Fig. 7 shows the normalized trajectories for the elbow and shoulder joint for the 360 actual lifts. It can be seen that a common pattern exists for each joint across different conditions. To model this common pattern exhibited by each joint, a polynomial trajectory model as in Eqs. (9)–(13) was developed for each joint by limiting the locations of the peak points (p_i, t_i) within a certain region, thus assuring the trajectories generated by each polynomial model have similar patterns as the actual trajectories. Specifically, a seventh order polynomial was used for the trajectories of the elbow, hip, knee, and ankle. An eighth-order polynomial was used for the shoulder trajectory.

5.2. Simulation results

Simulation was performed on the 360 lifts using the DPMS model. The actual initial and final postural configurations, the total duration of the lift, and the subject anthropometric characteristics were given to the model for each trial of simulation. Hsiang and Ayoub (1994) suggested the use of mean squared errors (MSE, Eq. (16)) and mean number of disconcordant pairs (MNDP, Eq. (17)) between the predicted trajectory and actual trajectory as two simulation performance indices.

$$\mathrm{MSE} = \frac{\sum_{i=1}^{n}[\theta(i) - \hat{\theta}(i)]^2}{n} \tag{16}$$

$$\mathrm{MNDP} = \frac{\sum_{i=1}^{N_1} f\{[\theta(i+1) - \theta(i)][\hat{\theta}(i+1) - \hat{\theta}(i)]\}}{n-1} \tag{17}$$

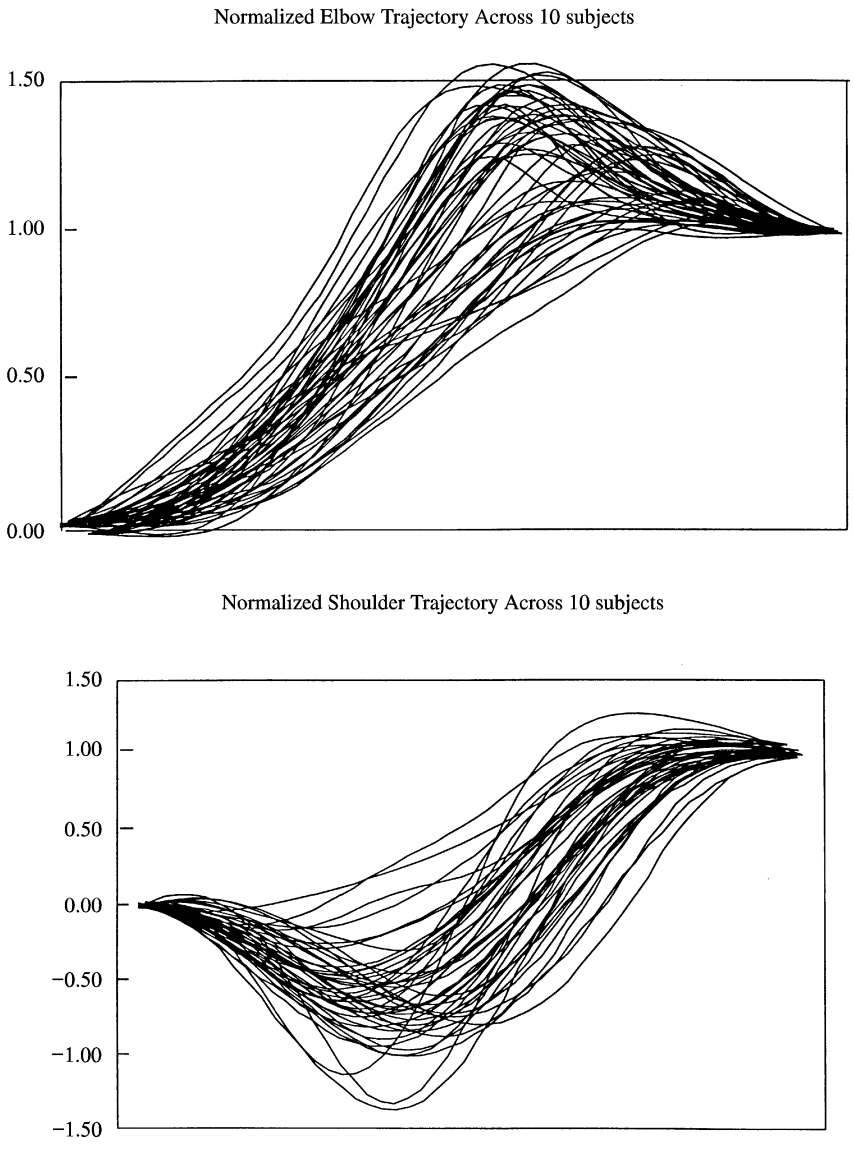

Fig. 7. Normalized trajectories for the elbow and shoulder across the 360 lifts.

where

$\theta(i)$ = actual position at time frame i,

$\hat{\theta}(i)$ = predicted position at time frame i,

$$f\{x\} = \begin{cases} 1, & x < 0, \\ 0, & \text{otherwise.} \end{cases}$$

The evaluation of the simulation model was made based on the two indices (Lin, 1995). Table 4 and Table 5 shows the MSE and MNDP, respectively, for both ranges (heights) of lift across all five joints for the 360 simulation lifts. A major improvement can be seen when compared to the previous study in Hsiang and Ayoub (1994). Fig. 8 shows the comparison between the actual and the predicted trajectory for subject 3 who performed three trials of floor-to-knuckle, large container, and

Table 4
Mean MSE (rad^2) for the two lifting heights, two container sizes, and three lifting weights for each joint

Height	*N*	Elbow	Shoulder	Hip	Knee	Ankle
Knuckle	180	0.016871	0.069770	0.016614	0.078842	0.0045651
Shoulder	180	0.047039	0.094682	0.031114	0.011587	0.0081531
Container						
Large	180	0.032051	0.086003	0.031144	0.035391	0.0069476
Small	180	0.031859	0.078449	0.016584	0.055038	0.0057707
Weight						
Heavy	120	0.037135	0.086020	0.021367	0.043981	0.0069642
Medium	120	0.031210	0.076891	0.022495	0.043341	0.0060834
Light	120	0.027520	0.083767	0.027731	0.048321	0.0060298

Table 5
Mean MNDP for the two lifting heights, two container sizes, and three lifting weights for each joint

Height	*N*	Elbow	Shoulder	Hip	Knee	Ankle
Knuckle	180	0.25159	0.24717	0.11077	0.18798	0.36191
Shoulder	180	0.11032	0.22166	0.09592	0.13401	0.39580
Container						
Large	180	0.17857	0.24433	0.09932	0.17313	0.36463
Small	180	0.18333	0.22449	0.10737	0.14887	0.39308
Weight						
Heavy	120	0.19303	0.23912	0.10833	0.15085	0.37381
Medium	120	0.18707	0.22177	0.10000	0.15816	0.38282
Light	120	0.16276	0.24235	0.10170	0.17398	0.37993

light-weight lifts. Fig. 9 shows the frame-to-frame stick diagrams for subject 2 (floor-to-knuckle, large container, and heavy weight lift trial) from the beginning to the end of the lift in percentage of total lifting duration. It is worth noting that the predicted lift tends to lag behind the actual in the first half of the lifting course, as shown in the figure. The actual lift was performed in a way that the load was picked up very quickly and brought closer to the body. The predicted lift does bring the load close to the body; however, the momentum of the load is usually smaller than the actual lifts at the initial stage of the lift.

The model predicts the lift-off stage with a slower speed can also be attributed to the assumption of the motionless start. As noted earlier, the initial velocities and accelerations of the joint movement were not zero. Although relatively small, they could affect the lift-off movement significantly.

A careful examination of the stick diagrams reveals that the model also lacks the fine movement coordination between joints. In most cases, the knee gets straight first, presumably trying to minimize the bending moments that occur at the knee. There seems to be a movement order for these joints. The lower body seems to begin with major movement prior to the upper extremities. Finally, from the trajectory plots (Fig. 8), one may also discover that the elbow moves up approximately the same time as the hip. The knee moves down

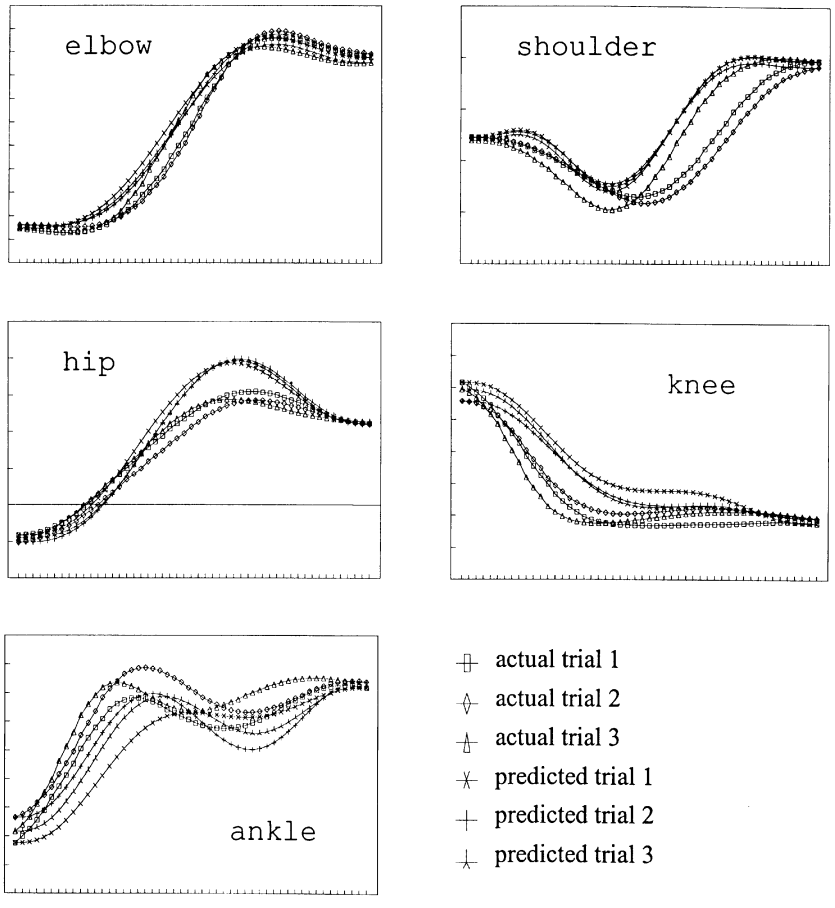

Fig. 8. The actual versus predicted trajectories for subject 3, performing three trials of floor-to-knuckle, large container, and light weight lift.

together with the shoulder then stays while the shoulder keeps moving up. Such patterns repeat again and again across all the lifts. The model does not handle the coordination problem directly but uses the pattern-fixed polynomials to address this problem. The biomechanical foundation of the joint movement coordination should be further studied to explain this consistent trajectory patterns.

6. Conclusion

The DPMS model predicts the two-dimensional joint motions for the lifting activities performed in the sagittal plane. Given the actual initial and final postural configurations, the anthropometric characteristics of the subject, and the task description, the model predicts the dynamic motion between the beginning and ending postures. Actual motion data were collected for a total of 360 lifts, including twelve different lifting tasks: the floor-to-knuckle and floor-to-shoulder ranges, the large and small containers, the heavy, medium, and light weights of load. The model was used to predict the motions of the 360 lifts. Comparisons were made between the actual motion and the predicted. The comparison indicated that the DPMS model simulates the lifting motion closely with good results.

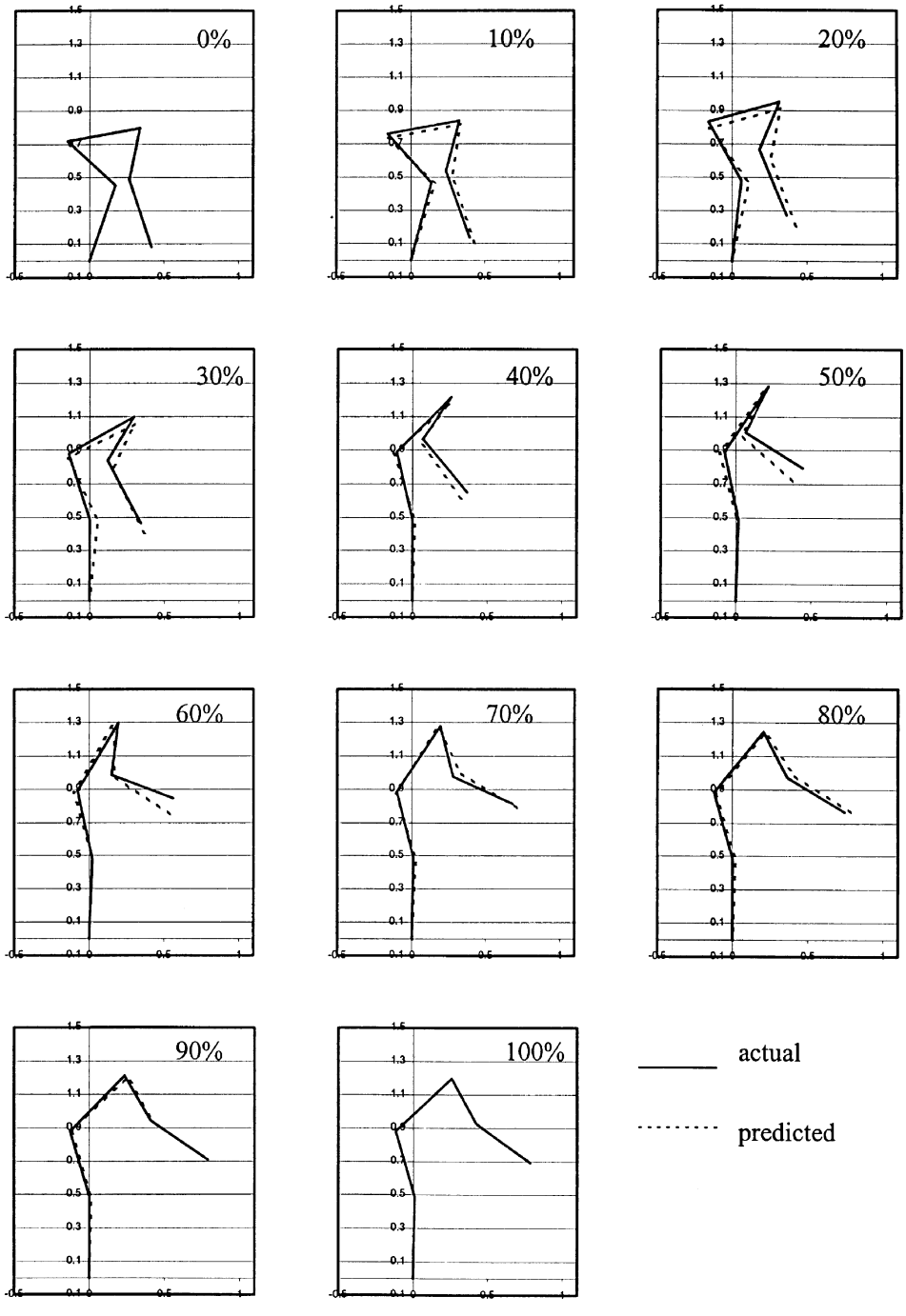

Fig. 9. Frame-to-frame stick diagrams for subject 2 (floor-to-knuckle, large container, and heavy weight) from the beginning to the end of the lift in percentage of total lifting duration.

Acknowledgements

This study was conducted at the Texas Tech University and was supported by a fund from NIOSH (No. RO1-OH02434).

References

Ayoub, M.A., 1971. A biomechanical model for the upper extremity using optimization techniques. Ph.D. Thesis. Texas Tech University, Lubbock.

Atkinson, K.E., 1989. In: An Introduction to Numerical Analysis. 2nd Ed., Wiley, New York, pp. 159–163.

Badler, N.I., Phillips, C.B., Webber, B.L., 1993. Simulating Humans, Computer Graphics Animation and Control. Oxford University Press, Oxford.

Chaffin, D.B., 1969. A computerized biomechanical model – development of and use in studying gross body actions. Journal of Biomechanics 2, 429–441.

Chaffin, D.B., Andersson, G.B.J., 1992. Occupational Biomechanics. 2nd Ed., Wiley, New York.

Fogleman, M., Smith, J.L., 1995. The use of biomechanical measures in the investigation of changes in lifting strategies over extended periods. International Journal of Industrial Ergonomics 16, 57–71.

Garg, A., Chaffin, D.B., Freivalds, A., 1982. Biomechanical stresses from manual load lifting: a static vs. dynamic evaluation. IIE Transactions 14 (4), 272–281.

Greenwood, D.T., 1988. Principles of Dynamics. 2nd Ed., Prentice-Hall, Englewood Cliffs, NJ.

Hatze, H., 1981. A comprehensive model for human motion simulation and its application to the take-Off phase of the long jump. Journal of Biomechanics 14 (3), 135–142.

Hsiang, M.S., 1992. Simulation of manual materials handling, Ph.D. dissertation, Texas Tech University.

Hsiang, S.H., Ayoub, M.M., 1994. Development of methodology in biomechanical simulation of manual lifting. International Journal of Industrial Ergonomics 13, 271–288.

Lasdon, L.S., Waren, A.D., 1979. Generalized reduced gradient software for linearly and nonlinearly constrained problems. In: Greenberg, H. (Ed.), Design and Implementation of Optimization Software. Sijthoff & Noordhoff, Alphen.

Lasdon, L.S., Waren, A.D., 1986. GRG2 User's Guide. School of Business Administration, University of Texas at Austin.

Lee, Y.H.T., 1988. An optimization approach to determine manual lifting motion, Ph.D. Thesis. Texas Tech University, Lubbock.

Leskinen, T.P.J., 1985. Comparison of static and dynamic biomechanical models. Ergonomics 28 (1), 285–291.

Lin, C.J., 1995. A computerized dynamic biomechanical simulation model for sagittal plane lifting activities. Ph.D. Dissertation, Texas Tech University.

Muth, M.B., 1976. An optimization model for the evaluation of lifting tasks. M.S. Thesis. North Carolina State University, Raleigh.

Muth, M.B., Ayoub, M.A., Gruver, W.A., 1978. A nonlinear programming model for the design and evaluation of lifting tasks. In: Drury, C.G. (Ed.), Safety in Manual Materials Handling, DHEW(NIOSH) Publication No. 78-185, pp. 96–109.

Petruno, M.J., 1972. A predictive model for motions of the arm in three-dimensional space. Ph.D. Thesis. Texas Tech University, Lubbock.

Stobbe, T.J., 1982. The development of a practical strength testing program for industry. Ph.D. Dissertation, The University of Michigan.

Subramanian, V., Hung, M.S., 1993. A GRG2-based system for training neural networks: design and computational experience. ORSA Journal on Computing 5 (4), 386–394.

The University of Michigan. 2D Static Strength Prediction Program, information from catalogue materials.

Townsend, M.A., Seireg, A., 1972. The synthesis of bipedal locomotion. Journal of Biomechanics 5, 71–83.

Yamaguchi, G.T., 1990. Performing whole-body simulations of gait with 3-D, dynamic musculoskeletal models. In: Winters, T.M., Woo, S.L.Y. (Eds.), Multiple Muscle Systems, Biomechanics and Movement Organization. Springer, Secaucus, NJ, pp. 663–679.